Int. J. Electrochem. Sci., 15 **(2020)** 7381 – 7389, doi: 10.20964/2020.08.25

International Journal of
ELECTROCHEMICAL
SCIENCE
www.electrochemsci.org

Novel and Promising Preparation of an Efficient Hematite Photoanode for Oxygen Evolution Reaction

Takahiro Murakami and Toshiyuki Abe[*]

Department of Frontier Materials Chemistry, Graduate School of Science and Technology, Hirosaki University, 3 Bunkyo-cho, Hirosaki 036-8561, Japan
[*]E-mail: tabe@hirosaki-u.ac.jp

Received: 6 March 2020 / *Accepted:* 30 April 2020 / *Published:* 10 July 2020

Iron(III) oxide (Fe_2O_3) has been recognized as a photoanode capable of water oxidation to dioxygen. For producing the efficient performance of Fe_2O_3 photoanode, the short-range diffusion of hole carriers and the ease of carrier recombination are the issues to be solved. Herein, a promising fabrication method for the preparation of an efficient α-Fe_2O_3 photoanode is presented. When α-Fe_2O_3 was subjected to acid treatment followed by loading of a co-catalyst, mix-valence cobalt(II,III) oxide (Co_3O_4), the double-treated Fe_2O_3 was superior to the untreated and acid-treated materials.

Keywords: Hematite; acid treatment; Co_3O_4; water oxidation; O_2 evolution

1. INTRODUCTION

Solar-driven hydrogen production from water has attracted significant attention as a clean and renewable energy source. The decomposition of water into H_2 and O_2 has been actively studied using both photoelectrochemical [1-7] and photocatalytic approaches [8-13]. To efficiently acquire solar-generated hydrogen, a wide range of the solar spectrum must be available to the water-splitting reaction. Iron(III) oxide (Fe_2O_3) is recognized as a typical photocatalyst that responds to visible-light energy (cf. band-gap: ca. 2.0–2.2 eV) [14-19], and can be fabricated by various methods (i.e. sintered single- and poly-crystalline preparation,[20,21] spray pyrolysis,[22] and atmospheric pressure chemical vapor deposition (APCVD) [23]). Water splitting by Fe_2O_3 has been investigated in terms of photoelectrochemistry because Fe_2O_3 alone cannot induce the overall reaction of water without applying biases to the reaction system. The conduction band of Fe_2O_3 corresponds to the reducing power and is potentially insufficient for H_2 formation. The aforementioned preparation methods have been used to form Fe_2O_3 nanoparticles, aiming at overcoming the short diffusion distance of the hole carrier [24-28] and the ease of carrier recombination. Recently, a novel preparation for an efficient

Fe_2O_3 photoanode was developed and involved acid treatment [29], which led to diminishing electron-hole recombination via increasing rates of detrapping photo-generated electrons based on the improved electrical conductivity in bulk. In addition, co-catalyst loading onto the photoanode (or photocatalyst) surface has been performed to efficiently generate O_2 from water in photoanodes composed of hematite [30-34]. Herein, a promising procedure for the preparation of an efficient Fe_2O_3 photoanode for O_2 evolution via double treatment is proposed. The procedure involves acid treatment and subsequent loading of a co-catalyst [i.e. cobalt(II, III) oxide denoted as Co_3O_4], which is a completely novel preparation procedure.

2. EXPERIMENTAL

A F-doped tin oxide (FTO)-coated glass plate (sheet resistance, 12 Ωcm^{-2}; FTO thickness, ca. 800 nm) was obtained from AGC Inc. and was utilized for the base electrode. All reagents used were of extra-pure grade and used as-received. Herein, α-Fe_2O_3 was prepared according to a previously reported procedure via spray pyrolysis [35]. First, a 0.5 M iron(III) chloride (Kanto Chemical) ethanolic solution was prepared and the resulting solution was sprayed 5 times to an FTO-coated face retained at 400°C. This operation was performed thrice at 5 min intervals. The final α-Fe_2O_3 product was obtained by sintering the aforementioned sample at 400°C for 2 h in an electric furnace (Yamato Scientific, FO300; temperature ramp rate, 2°C/min.). The resulting α-Fe_2O_3 is hereafter abbreviated as FTO/α-Fe_2O_3.

Subsequently, the FTO/α-Fe_2O_3 was subjected to acid treatment [29], wherein an Fe_2O_3 face (geometrical area: 2 × 3 cm) was soaked in a 1 M phosphoric acid solution for 3 min. The treated α-Fe_2O_3 was later washed with deionized water and dried under an air atmosphere. The materials were then sintered at 450°C for 2 h in an electric furnace at a ramp rate of 2°C/min. The acid-treated α-Fe_2O_3 is referred to as FTO/AT-α-Fe_2O_3.

The loading of Co_3O_4 co-catalyst onto FTO/AT-α-Fe_2O_3 was achieved according to the method described by Lim et al. [36]. A methanol solution (10 mL in total) containing 2-aminoethanol (0.1 mL) was prepared and 5 mg of cobalt(II) acetylacetonate (Tokyo Kasei) was dissolved in the aforementioned methanolic solution, followed by stirring for 24 h. The precursor solution (100 µL) of Co complex was dropped onto the Fe_2O_3 surface in FTO/AT-α-Fe_2O_3, and subsequently spin-coated for 30 s (rotation speed: 2000 rpm). Co_3O_4 loading was completed by sintering at 350°C for 15 min and the double-treated α-Fe_2O_3 is denoted as FTO/AT-α-Fe_2O_3/Co_3O_4.

The absorption spectra of FTO/α-Fe_2O_3, FTO/AT-α-Fe_2O_3 and FTO/AT-α-Fe_2O_3/Co_3O_4 were measured using a PerkinElmer Lambda 35 spectrophotometer. The untreated and treated α-Fe_2O_3 surfaces were observed by scanning electron microscopy (SEM; JEOL, JSM-7000F). Photoelectrochemical measurements, including cyclic voltammograms and photocurrents for acquiring action spectra, were performed using a single-compartment cell composed of modified FTO working (effective area: 1 × 1 cm), spiral Pt wire counter, and Ag/AgCl (in saturated KCl electrolyte) reference electrodes (Scheme 1).

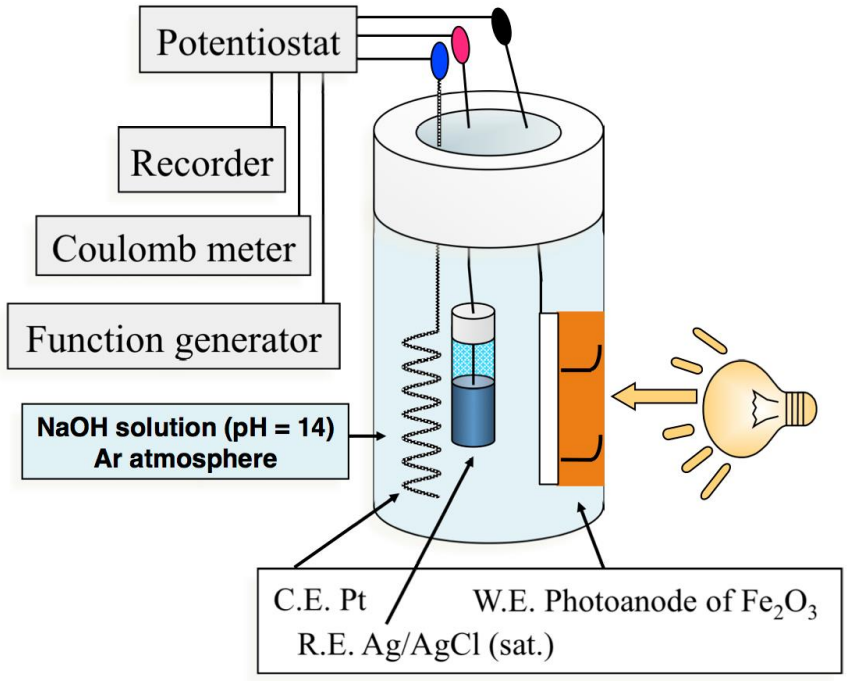

Scheme 1. An illustration of a three-electrode system used in the present work.

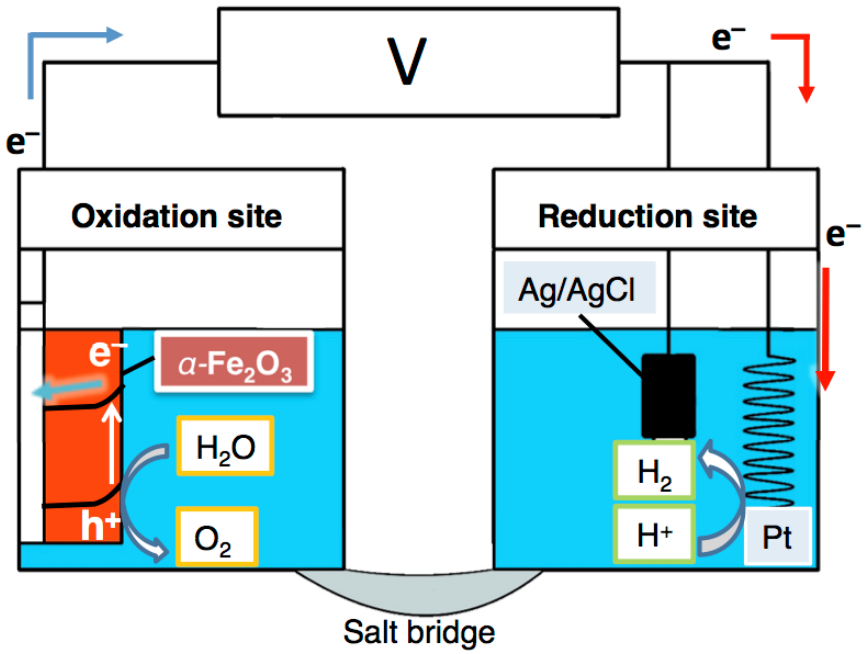

Scheme 2. Schematic illustration of the cell used for the water-splitting reaction.

For these measurements, an alkaline solution (pH 14) containing NaOH was used as the electrolyte solution. Photoelectrochemical experiments were operated using a potentiostat (Hokuto Denko, HA-301) with function generator (Hokuto Denko, HB-104), coulomb meter (Hokuto Denko, HF-201), and data logger (GRAPHTEC, midi LOGGER GL900) under illumination. A xenon lamp

(light intensity: ca. 70 $mW \cdot cm^{-2}$) was used to irradiate the α-Fe_2O_3 photoanodes. The light intensity was measured using power meters (CS-40, ASAHI SPECTRA; type 3A, Ophir Japan, Ltd). When acquiring the action spectra for photocurrents, a light source was combined with a monochromator (Soma Optics, Ltd., S-10) to irradiate monochromatic light.

Photoelectrochemical water decomposition was performed using a twin-compartment cell separated by a salt bridge (Scheme 2). The modified FTO (oxidation site) and Pt wire (reduction site) were placed in each compartment, and an Ag/AgCl reference electrode was co-located with the Pt counter electrode. The α-Fe_2O_3 photoanode was immersed in an alkaline solution (pH 14) and the other electrodes were placed in a phosphoric acid solution (pH 2). To prepare the salt bridge, agar (1.3 g) and KNO_3 (4.74 g) were first dissolved in hot water (10 mL) and the mixture was then allowed to flow into the bridging part of the cell, solidifying at room temperature. Gaseous products (i.e. O_2 and H_2) were analyzed using a gas chromatograph (GL Sciences, GC-3200) equipped with a thermal conductivity detector (column, 5 Å molecular sieve; carrier gas, argon).

Calculation methods of incident photon-to-current efficiency (*IPCE*) as well as faradaic efficiency (*F.E.*) have been described elsewhere [6,7].

3. RESULTS AND DISCUSSION

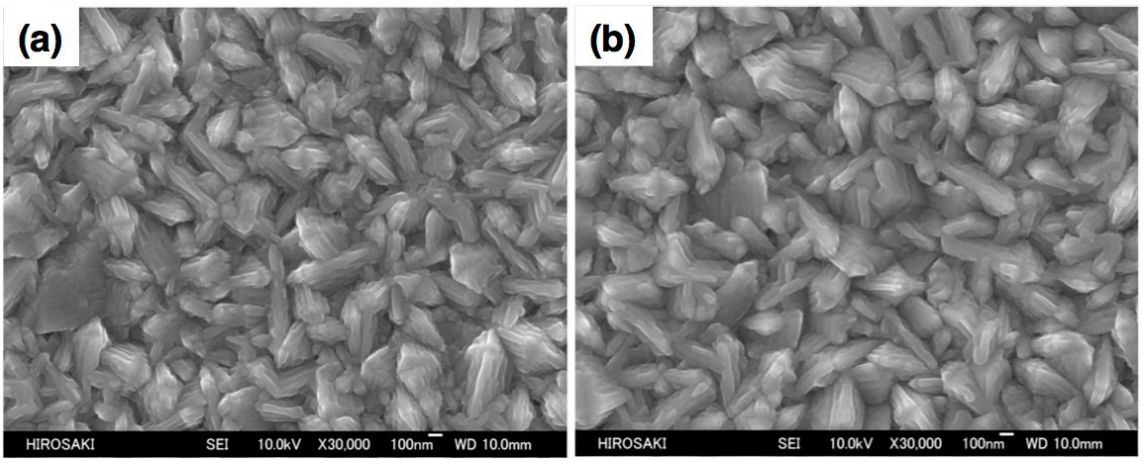

Figure 1. SEM images of α-Fe_2O_3 before (a) and after (b) acid treatment.

Fig. 1 shows the obtained SEM images of the α-Fe_2O_3 surfaces with and without acid treatment (i.e. FTO/AT-α-Fe_2O_3 and FTO/α-Fe_2O_3). Regardless of the α-Fe_2O_3 treatment, those surfaces remained unchanged. Moreover, no crystal size changes were observed. This type of morphological immutability before and after the treatment has been previously reported by Cowan and Li [29]. Based on the Tauc plot originating from the absorption spectrum of α-Fe_2O_3 (Fig. 2), the band gap energy (E_g) of the resulting α-Fe_2O_3 was estimated to be ca. 2.0 eV, consistent with previously reported data (*vide supra*) [14-19]. In addition, the magnitude of the band gap remained constant irrespective of the acid treatment.

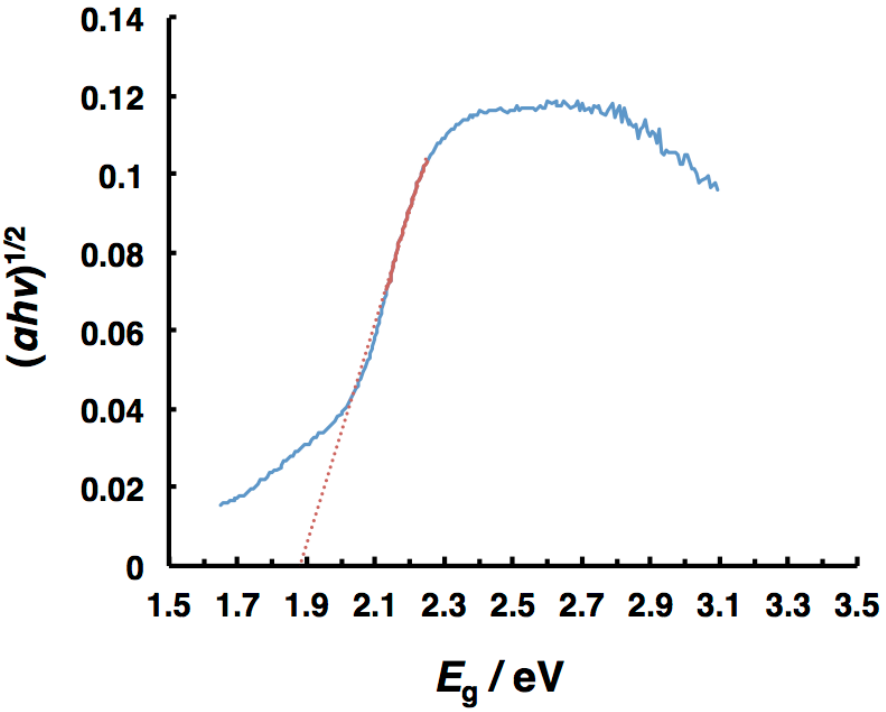

Figure 2. Tauc plot originating from the absorption spectrum of untreated α-Fe_2O_3. The terms, α, h and ν represent absorption coefficient, Planck constant, and frequency of light, respectively.

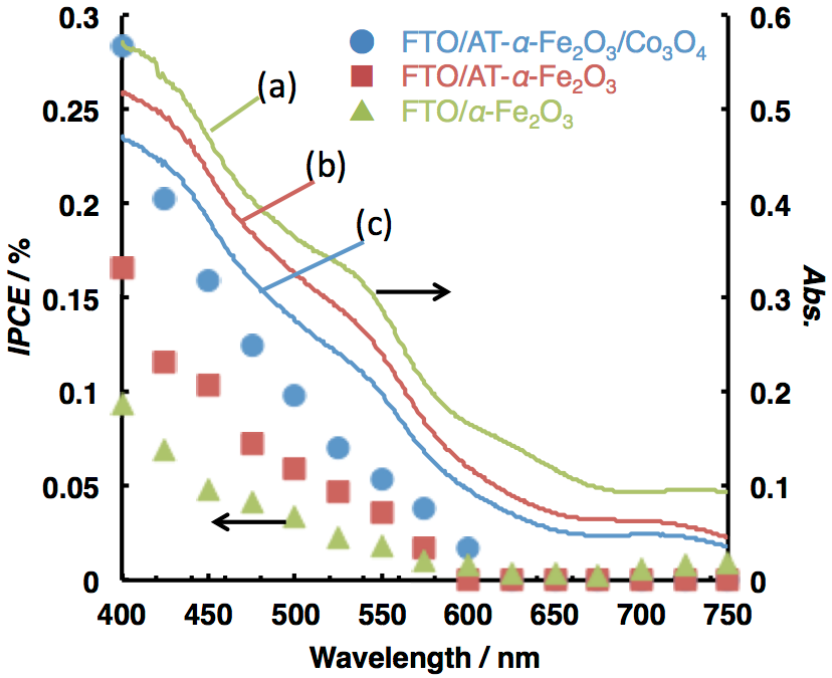

Figure 3. Action spectra for the photocurrents at the α-Fe_2O_3 photoanodes. Solid lines indicate the absorption spectra of α-Fe_2O_3: (a) FTO/α-Fe_2O_3; (b) FTO/AT-α-Fe_2O_3; and (c) FTO/AT-α-Fe_2O_3/Co_3O_4.

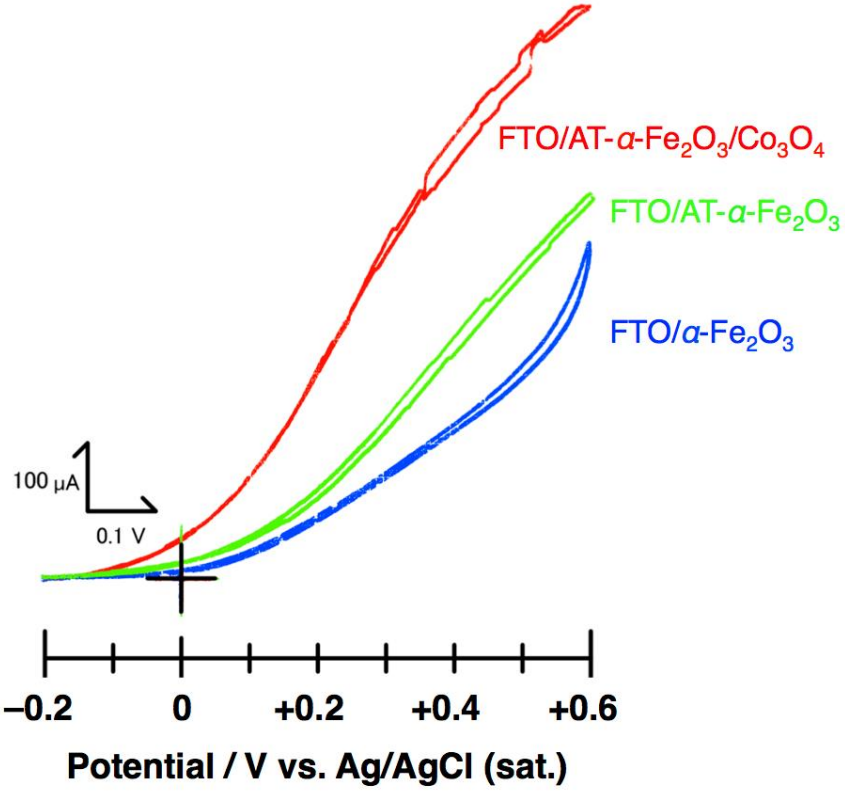

Figure 4. Cyclic voltammograms of three types of α-Fe_2O_3 used in the present study. Working electrode: FTO/α-Fe_2O_3, FTO/AT-α-Fe_2O_3, or FTO/AT-α-Fe_2O_3/Co_3O_4; reference electrode: Ag/AgCl (sat.); counter electrode, Pt wire; electrolyte solution: NaOH solution (pH = 14); light intensity: 70 mW/cm^2; Scan rate: 20 mV/s.

Table 1 Data for the photoelectrochemical water splitting using three types of α-Fe_2O_3 as photoanodes at an applied potential of +0.2 V vs. Ag/AgCl[a)]

Types of photoanodes	The amounts of gaseous products / μL	
	H_2	O_2
FTO/α-Fe_2O_3	43.4	21.9
FTO/AT-α-Fe_2O_3	71.7	36.4
FTO/AT-α-Fe_2O_3/Co_3O_4	157	77.1

a) irradiation time, 3 hours

Three types of α-Fe_2O_3 photoanodes, i.e. FTO/α-Fe_2O_3, FTO/AT-α-Fe_2O_3, and FTO/AT-α-Fe_2O_3/Co_3O_4, induced O_2 evolution, resulting in the generation of photoanodic currents (*vide infra*). Fig. 3 shows the action spectra for photocurrents at the α-Fe_2O_3 photoanodes compared to the absorption spectra of α-Fe_2O_3. In each case, the photocurrents were confirmed at wavelengths of <600

nm, corresponding to the absorption edge of α-Fe_2O_3 (*vide supra*). For the typical data at 400 nm, the *IPCE* value of FTO/AT-α-Fe_2O_3/Co_3O_4 was ca. 1.5 and 3 times higher than that of FTO/AT-α-Fe_2O_3 and FTO/α-Fe_2O_3, respectively. This demonstrated that the double treatment is most effective for fabricating an efficient photoanode composed of α-Fe_2O_3. Analogous photoelectrode performances were confirmed via the voltammograms (Fig. 4).

Table 2 Data for the photoelectrochemical water splitting using three types of α-Fe_2O_3 as photoanodes at an applied potential of +0.6 V vs. Ag/AgCl[a)]

Types of photoanodes	The amounts of gaseous products / μL	
	H_2	O_2
FTO/α-Fe_2O_3	130	64.3
FTO/AT-α-Fe_2O_3	289	141
FTO/AT-α-Fe_2O_3/Co_3O_4	405	213

a) irradiation time, 3 hours

The photoelectrochemical decomposition of water was achieved by applying low and high potentials to the reaction, as shown in Table 1 and Table 2. In each case, the stoichiometric formation of O_2 and H_2 was observed (cf. *F.E.*, >85% for both O_2 and H_2 formation). Furthermore, applying a high potential to the reaction system resulted in relatively higher amounts of O_2 and H_2, owing to efficient charge separation resulting in increasing amounts of carriers available for the water-splitting reaction. This potential-dependent water splitting has been observed in previous studies [6,7,37-40]. The photoelectrolysis data clearly demonstrated the positive effects of the single and double modification of α-Fe_2O_3, similar to the aforementioned photoelectrochemical results (*vide supra*). First, FTO/AT-α-Fe_2O_3 was superior to FTO/α-Fe_2O_3. The short-distance diffusion of hole carrier in α-Fe_2O_3 has been shown to induce inefficient charge separation [24-28]; however, as described by Cowan and Li [29], the acid treatment of α-Fe_2O_3 improves its electrical conductivity, thereby enhancing the transport efficiency of surface-trapped electrons towards the bulk by surface passivation, diminishing electron and hole carrier recombination, and leading to an increased amount of holes available for O_2 evolution. In addition, in some cases of O_2 evolution at the α-Fe_2O_3 photoanode, Co_3O_4 has been applied as a co-catalyst [41,42]. The mixed-valence Co_3O_4 contains Co^{2+} ions that function as hole-trapped sites. Co_3O_4 loading further enhances the charge separation, leading to efficient O_2 evolution via catalysis of the Co^{3+} ions generated under irradiation [36].

4. CONCLUSION

Herein, a novel α-Fe_2O_3 photoanode was prepared for the efficient evolution of O_2. Acid treatment of α-Fe_2O_3 was effective; following the loading of a Co_3O_4 co-catalyst, O_2 evolution was

further enhanced. The α-Fe_2O_3 employed was prepared by a conventional method (i.e. spray pyrolysis). Irrespective of the fabrication method of α-Fe_2O_3, the double treatment is a promising and ubiquitous process for preparing an efficient α-Fe_2O_3 photoanode.

ACKNOWLEDGEMENTS
This work was partly supported by a grant from Yashima Environment Technology Foundation and the Cooperative Research Program of "Network Joint Research Center for Materials and Devices".

References

1. C.D. Windle, H. Kumagai, M. Higashi, R. Brisse, S. Bold, B. Jousselme, M. Chavarot-Kerlidou, K. Maeda, R. Abe, O. Ishitani and V. Artero, *J. Am. Chem. Soc.*, 141 (2019) 9593.
2. K. Wang, D. Huang, L. Yu, K. Feng, L. Li, T. Harada, S. Ikeda and F. Jiang, *ACS Catal.*, 9 (2019) 3090.
3. A. Kawde, A. Annamalai, A. Sellstedt, P. Glatzel, T. Wågberg and J. Messinger, *Dalton Trans.*, 48 (2019) 1166.
4. T. Higashi, H. Nishiyama, Y. Suzuki, Y. Sasaki, T. Hisatomi, M. Katayama, T. Minegishi, K. Seki, T. Yamada and K. Domen, *Angew. Chem. Int. Ed.*, 58 (2019) 2300.
5. D. Shao, L. Zheng, D. Feng, J. He, R. Zhang, H. Liu, X. Zhang, Z. Lu, W. Wang, W. Wang, F. Lu, H. Dong, Y. Cheng, H. Liu and R. Zheng, *J. Mater. Chem. A*, 6 (2018) 4032.
6. Y. Kawai, K. Nagai and T. Abe, *RSC Adv.*, 7 (2017) 34694.
7. T. Abe, K. Fukui, Y. Kawai, K. Nagai and H. Kato, *Chem. Commun.*, 52 (2016) 7735.
8. A. Fujishima and K. Honda, *Nature*, 238 (1972) 37.
9. Y. He, M. Zhang, J.J. Shi, Y.L. Cen and M. Wu, *J. Phys. Chem. C*, 123 (2019) 12781.
10. S. Chen, G. Ma, Q. Wang, S. Sun, T. Hisatomi, T. Higashi, Z. Wang, M. Nakabayashi, N. Shibata, Z. Pan, T. Hayashi, T. Minegishi, T. Takata and K. Domen, *J. Mater. Chem. A*, 7 (2019) 7415.
11. K.W. Park and A.M. Kolpak, *J. Mater. Chem. A*, 7 (2019) 6708.
12. R. Peng, Y. Ma, B. Huang and Y. Dai, *J. Mater. Chem. A*, 7 (2019) 603.
13. H. He, J. Cao, M. Guo, H. Lina, J. Zhang, Y. Chene and S. Chena, *Appl. Catal. B*, 249 (2019) 246.
14. X. Xie, K. Li and W.D. Zhang, *RSC Adv.*, 6 (2016) 74234.
15. W.D. Chemelewski, O. Mabayoje, D. Tang, A.J.E. Rettie and C.B. Mullins, *Phys. Chem. Chem. Phys.*, 18 (2016) 1644.
16. A.B.F. Martinson, M.J. DeVries, J.A. Libera, S.T. Christensen, J.T. Hupp, M.J. Pellin and J.W. Elam, *J. Phys. Chem. C*, 115 (2011) 4333.
17. *H. Wang and J.A. Turner, J. Electrochem. Soc.,* 157 *(2010)* F173.
18. R. Schrebler, K. Bello, F. Vera, P. Cury, E. Muñoz, R. del Río, H.G. Meier, R. Córdova and E.A. Dalchiele, *Electrochem. Solid-State Lett.,* 9 *(2006)* C110.
19. S. Kakuta and T. Abe, *J. Mater. Sci.*, 44 (2009) 2890.
20. C. Sanchez, K.D. Sieber and G.A. Somorjai, *J. Electroanal. Chem.*, 252 (1988) 269.
21. R. Shinar and J.H. Kennedy, *Sol. Energy Mater.*, 6 (1982) 323.
22. A.S.N. Murthy and K.N. Reddy, *Mater. Res. Bull.*, 19 (1984) 241.
23. I. Cesar, A. Kay, J.A.G. Martinez and M. Grätzel, *J. Am. Chem. Soc.*, 128 (2006) 4582.
24. M.P. Dare-Edwards, J.B. Goodenough, A. Hamnett and P.R. Trevellick, *J. Chem. Soc. Faraday Trans.*, 79 (1983) 2027.
25. J.H. Kennedy and K.W. Frese, *J. Electrochem. Soc.*, 125 (1978) 709.
26. J.Y. Kim, G. Magesh, D.H. Youn, J.W. Jang, J. Kubota, K. Domen and J.S. Lee, *Sci. Rep.*, 3 (2013) 2681.

27. F. Le Formal, N. Tetreault, M. Cornuz, T. Moehl, M. Grätzel and K. Sivula, *Chem. Sci.*, 2 (2011) 737.
28. K. Sivula, F. Le Formal and M. Grätzel, *ChemSusChem*, 4 (2011) 432.
29. Y. Yang, M. Forster, Y. Ling, G. Wang, T. Zhai, Y. Tong, A.J. Cowan and Y. Li, *Angew. Chem. Int. Ed.*, 55 (2016) 3403.
30. A. Subramanian, M.A. Mahadik, J.W. Park, I.K. Jeong, H.S. Chung, H.H. Lee, S.H. Choi, W.S. Chae and J.S. Jang, *Electrochim. Acta*, 319 (2019) 444.
31. F. Li, J. Li, L. Gao, Y. Hu, X. Long, S. Wei, C. Wang, J. Jin and J. Ma, *J. Mater. Chem. A*, 6 (2018) 23478.
32. C. Du, J. Wang, X. Liu, J. Yang, K. Cao, Y. Wen, R. Chen and B. Shan, *Phys. Chem. Chem. Phys.*, 19 (2017) 14178.
33. J. Wang, J. Su and L. Guo, *Chem. Asian J.*, 11 *(2016)* 2328.
34. J.Y. Zheng, S.I. Son, T.K. Van and Y.S. Kang, *RSC Adv.*, 5 (2015) 36307.
35. S.U.M. Khan and J. Akikusa, *J. Phys. Chem. B*, 103 (1999) 7184.
36. C.S. Chua, D. Ansovini, C.J.J. Lee, Y.T. Teng, L.T. Ong, D. Chi, T.S. Andy Hor, R. Raja and Y.F. Lim, *Phys. Chem. Chem. Phys.*, 18 (2016) 5172.
37. W. Zhao, Z. Wang, X. Shen, J. Li, C. Xu C and Z. Gan, *Int. J. Hydrogen Energy*, 37 (2012) 908.
38. M. Moriya, T. Minegishi, H. Kumagai, M. Katayama, J. Kubota and K. Domen, *J. Am. Chem. Soc.*, 135 (2013) 3733.
39. Y. Hou, F. Zuo, A.P. Dagg, J. Liu and P. Feng, *Adv. Mater.*, 26 (2014) 5043.
40. I. Fujimoto, N. Wang, R. Saito, Y. Miseki, T. Gunji and K. Sayama, *Int. J. Hydrogen Energy*, 39 (2014) 2454.
41. P. Zhang, T. Wang, X. Chang, L. Zhang and J. Gong, *Angew. Chem. Int. Ed.*, 55 (2016) 5851.
42. R.R. Devarapalli, C.K. Kamaja and M.V. Shelke, *ChemistrySelect*, 2 (2017) 2544.